NJC

Accepted Manuscript

This article can be cited before page numbers have been issued, to do this please use: O. Rezazgui, P. Trouillas, S. Qiu, B. Siegler, J. Gierschner and S. Leroy-Lhez, *New J. Chem.*, 2016, DOI: 10.1039/C5NJ02901E.

View Article Online
DOI: 10.1039/C5NJ02901E

New Journal of Chemistry

ARTICLE

Synthesis and Conformation of a Novel Fluorescein-Zn-Porphyrin Dyad and Intramolecular Energy Transfer

Received 00th January 20xx,
Accepted 00th January 20xx

DOI: 10.1039/x0xx00000x

www.rsc.org/

Olivier Rezazgui,[a] Patrick Trouillas,[b,c],* Shi-hong Qiu,[a] Benjamin Siegler,[d] Johannes Gierschner,[e] Stephanie Leroy-Lhez[a]*

This study describes the synthesis and characterization of a new zinc porphyrin-fluorescein dyad, the two chromophoric units being covalently linked by a 1,2,3-triazole bridge. The latter was formed by a Cu-catalyzed Huisgen 1,3-dipolar cycloaddition. The conformational analysis of this dyad (**1**) was performed by NOESY experiments, suggesting interactions between moieties; density functional theory (DFT) calculations confirmed clear evidence of a folded conformer, which is stabilized by electrostatic and CH-π interactions. Photophysical measurements demonstrated solvent-dependent energy transfer, with efficiency of about 40%.

Introduction

Over the past twenty years, porphyrins have extensively been studied as an important class of molecules in biology and materials science. They are naturally involved in various key biological processes such as photosynthesis in plants[1] or oxygen transport in the blood.[2] They have also a broad range of applications. For example, synthesized porphyrins can be used in analytical chemistry,[3] in organic solar cells as energy transfer systems,[4,5] in oxidation catalysis,[6] in health (photodynamic therapy for cancers and other diseases treatment, antimicrobial activity)[7–9] and more surprisingly in agriculture as potential photoactivable herbicides,[10,11] pesticides[12] and insecticides.[13,14] These two last applications are based on the ability of porphyrins, after photoactivation, to produce reactive oxygen species by interaction with surrounding substrate or oxygen. As biodiversity, environment preservation and health safety are the main challenges of agronomy, search for new active herbicides that are plant-specific, non-toxic to wildlife, biodegradable by microorganisms and non-polluting groundwater is thus primordial. In that respect porphyrins seem to be good candidates to meet these multiple expectations.

In the recent years, numerous studies have been devoted to the design of new porphyrin derivatives to optimize their physical (*e.g.*, redox, optical…) properties according to one of these applications. An interesting approach consists of modulating them by covalently linking to another unit such as electron donor and/or acceptor, chromophore or two-photon absorber antenna.[15–18] Due to the current energy context, the majority of the studies on dyads containing porphyrins focus on energy transfer and conversion.[19] Without being exhaustive, two major areas stand out. First, the synthesis of dyads in which porphyrins play the role of electron donor (often coupled to molecules like fullerenes) in order to promote electron transfer for the development of new organic photovoltaic devices.[7,20–25] Second, multichromophoric systems based on porphyrins are designed as artificial photosynthetic systems.[26–31]

Although porphyrins are very often studied as dyads, there are only a handful of publications on labeling with a fluorescent molecule, without intention to establish interactions between the two patterns, for environmental and/or health applications. For example, porphyrin-rhodamine[32] and porphyrin-fluorescein[33,34] dyads have already been synthesized, but without intention of using them under biological conditions. The interest of such association is particularly relevant as porphyrin itself exhibits very low fluorescence quantum yields (*ca*. 0.1),[35] whereas this property is crucial for visualization and tracking in biological media. Moreover, due to similar chemical structure, porphyrins have similar optical properties than chlorophyll and thus, this is an additional serious drawback to localize them in plants without using an appropriate fluorescent tag. To properly label porphyrins is thus critical agronomic issue to facilitate their use as photo-herbicide and/or pesticides.

Designing of molecular systems based on association of a porphyrin unit to a fluorescent tag appears as a novel, suitable solution to develop new kind of biodegradable herbicides. However, although the study in plants is the ultimate goal, it is first necessary to use an optimized molecular design step to obtain the most appropriate structures and eliminate all phenomena that can interfere. In that purpose, we describe here the synthesis and characterization of a new Zn-porphyrin-fluorescein dyad (**1**), in which both chromophoric units are linked by a triazole bridge, as well as of spectroscopic references **2** and **3** (Scheme 1). NOESY studies suggest interactions between the porphyrin and fluorescein moieties, which are then supported by density functional theory (DFT) calculations.

[a] *LCSN EA1069, Univ. Limoges, 123 Avenue Albert Thomas, 87060 Limoges, France.*
[b] *INSERM UMR 850, Univ. Limoges, School of Pharmacy, 2 rue du Docteur Marcland, 87025 Limoges Cedex, France.*
[c] *Regional Centre of Advanced Technologies and Materials, Department of Physical Chemistry, Faculty of Science, Palacký University, tř. 17 listopadu 12, 771 46 Olomouc, Czech Republic.*
[d] *PIAM, Université d'Angers, LUNAM Université, Angers, France.*
[e] *Madrid Institute for Advanced Studies - IMDEA Nanoscience, C/ Faraday 9, Ciudad Universitaria de Cantoblanco, E-28049 Madrid, Spain.*

Electronic Supplementary Information (ESI) available: [Materials, instrumentations and results of theoretical calculations (molecular orbitals analysis and matrix)]. See DOI: 10.1039/x0xx00000x

View Article Online
DOI: 10.1039/C5NJ02901E

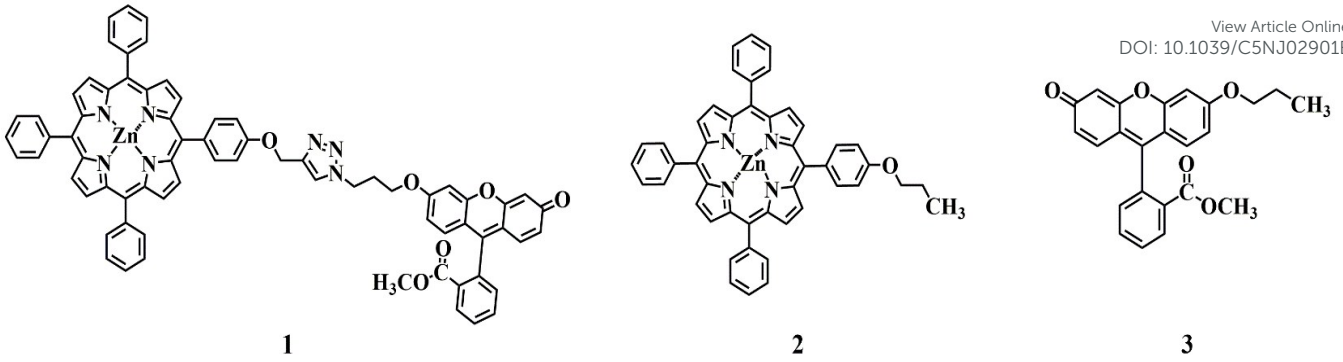

Scheme 1: Structure of dyad **1** and reference compounds **2** and **3**

Steady-state and time-resolved fluorescence spectroscopy investigation provided evidence for energy transfer between the fluorescein and the porphyrin moiety in the dyad.

Results and discussion

Synthesis

The synthesis of dyad **1** has required preliminary synthesis of both porphyrin **6** and fluorescein **10** precursors. Compound **6** was obtained in three step (Scheme 2), the first one being the formation of the macrocycle according to Little's method[36] by reaction between 1 equiv. of 4-hydroxybenzaldehyde, 3 equiv. of benzaldehyde and 4 equiv. of pyrrole. Compound **4** was then obtained after purification step to remove other porphyrinic compounds formed, with 7% yield, in agreement with the literature.[37,38] Synthesis of **4** was also carried out by microwave irradiations under milder conditions but with equivalent yields (6-8%).[39] Little's method was preferred to those using dipyrromethanes[40] as starting compounds are commercially available and this synthesis corresponds to a routine one.

Then, as a second step, propargylation of the hydroxyl group of **4** was conducted through a Williamson's reaction in the presence of 20 equiv. of propargyl bromide to afford intermediate **5** with 79% yield. The third step consisted of a zinc metallation of the porphyrin nucleus. This was of upmost importance because **1** was obtained by a click-chemistry reaction catalyzed by copper(I)[41] between **6** and **10**. As this metal exhibits high affinity to the porphyrin nucleus, there is a risk of copper complexation by the porphyrin moiety, which may decrease the efficiency of catalysis and hence reaction yields. Moreover, as described by Figueiredo *et al*. in 1999,[42] the production of reactive oxygen species (ROS) was dramatically decreased in copper-porphyrin whereas zinc-porphyrins are known to be efficient ROS producers.[42] Therefore metalation of **5** was done by the reaction of 10 equiv. of Zinc(II) acetate in a mixture of methanol and chloroform (v/v). Compound **6** was then obtained in quantitative yield (≥ 99%). For the sake of comparison in spectroscopic studies, a porphyrin of reference **2** was also synthesized, performing a Williamson's reaction on **4** (using excess of 1-bromopropane) / metalation sequence (78% yield for the two steps).

In parallel, the fluorescein precursor **10**, required for synthesis of **1**, was obtained in three steps from fluorescein (Scheme 3). The first step was a simple esterification of the commercial fluorescein[43] affording intermediate **8** in quantitative yield. This step has allowed blocking the carboxylic function in order to prevent lactone formation.[43] Then compound **9** was obtained by alkylation of **8** with an excess of 1,3-dibromopropane (64% yield) and subsequently transformed, into **10** by reaction with sodium azide based on Singh *et al.* method (quantitative yield).[44] As for the porphyrin moiety, a fluorescein-based reference (**3**) was synthesized by an easy Williamson's reaction with an excess of 1-bromopropane (89% yield) performed on **8**.

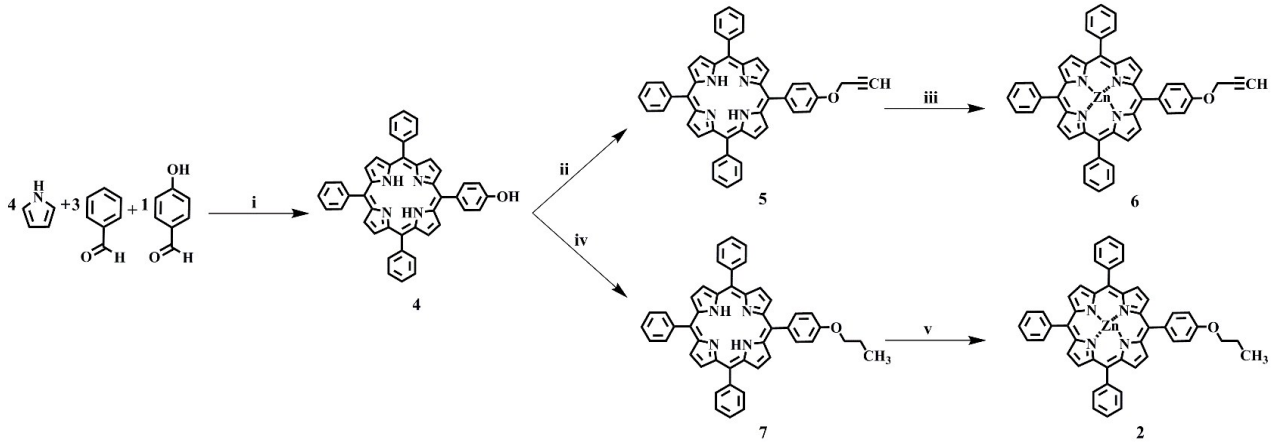

Scheme 2: Reagents and conditions: i) propionic acid, 120°C, 2h, 7%.; ii) propargyl bromide, K_2CO_3, dry DMF, Ar, 24h, 79%; iii) Zn(II)acetate, $CHCl_3$/MeOH (v/v), one night, >99%; iv) 1-bromopropane, K_2CO_3, dry DMF, 2x 5 min./ 200 W/ 120°C, 78%; v) Zn(II)acetate, $CHCl_3$/MeOH (v/v), one night, >99%.

View Article Online
DOI: 10.1039/C5NJ02901E

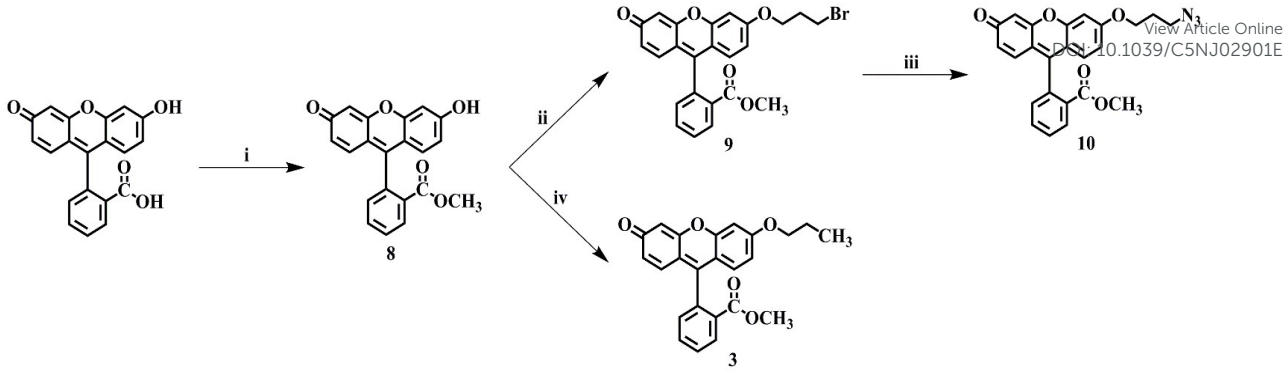

Scheme 3: Reagents and conditions: i) MeOH, sulfuric acid, 18h, 98%.; ii) dibromopropane, K_2CO_3, dry DMF, Ar, 20h, 64%; iii) sodium azide, dry DMF, Ar, 24h, >99%; iv) 1-bromopropane, K_2CO_3, dry DMF, Ar, 18h, 89%.

The porphyrin and fluorescein key-moieties (**6** and **10**) were then coupled by an Azide-Alkyne [2+3] Huisgen Cycloaddition[41,45–47] using Copper(II) acetate/sodium ascorbate (2.7/7 equiv.) as catalytic system (acting as precursor of the real catalytic specie, namely Copper(I), produced *in situ*) (Scheme 4). During this coupling step, the solubility of the various reagents was problematic. To overcome this issue, salts (Copper (II) acetate and sodium ascorbate) were dissolved together in distillated water whereas the two precursors (**6** and **10**), were dissolved in THF. Afterwards, the two solutions were mixed. After 24h reaction at room temperature, **1** was obtained with 91% yield.

In order to reach spectroscopic purity, **1** was purified repeatedly on silica gel column (twice) then on preparative plates (three times). Also, before each spectral analysis, a final purification on preparative plates using spectroscopic solvent as eluent was performed. The (UV-Vis absorption, fluorescence emission and excitation) spectra, lifetimes and fluorescence quantum yields were reproducible.

Conformational analysis

The conformational features of both porphyrin and fluorescein moieties have been extensively described, mainly stressing planarity as being responsible for their photophysical properties.[48] Distortion from planarity has been described for porphyrins depending on the central metal, substituents and environmental conditions.[49,50] In fluorescein, only the xanthen-3-one moiety is fully planar, whereas the phenyl ring is almost perpendicular to the former. In the dyad, both nature and length of the linker are key elements, determining conformation and thus electronic interactions between both chromophores, which should have a pronounced effect especially on energy transfer between the porphyrin and fluorescein moieties (*vide infra*).

For the novel dyad **1**, we chose a methoxy-triazole-propyloxy linker as this pattern was known to be stable in biological medium and non-toxic, and easy to synthesize.[51] Moreover, the linker should be stiff enough to restrict the conformational space to a few possible stable geometries. As often observed in such systems bearing two separate chromophores, folding is likely to occur, providing two types of conformers.

To investigate the presence of folded *vs*. linear conformations, we conducted temperature dependent ^{1}H-NMR studies of **1** in $CDCl_3$ between 233K and 333K. Porphyrin hydrogen peaks were seen as broad signals at high temperature, which sharpened and split as temperature was lowered, possibly revealing the presence of different conformers undergoing fast exchange at high temperature. NOESY spectra were therefore performed at 253K and 323K in order to see possible spatial proximity between both the porphyrin and the fluorescein moieties. The NOESY spectrum obtained at low-temperature showed correlation spots between some protons of xanthen-3-one moiety of fluorescein (at 6.7 ppm) and of porphyrin (at 7.9 ppm and 8.9 ppm), revealing a folded geometry of the dyad (Figure 1). Those correlation spots were absent in the high-temperature spectrum, probably due to fast exchanges between the conformers (*vide infra* for thorough discussion).

To support these experimental evidences and to clearly describe conformers, a DFT-based conformational analysis was conducted. This was assessed by using both the standard B3LYP (that does not include dispersion) and the ωB97XD (that includes both dispersion and long-range corrections) exchange-correlation (XC) functionals.[52,53] Full geometry optimizations were performed in the gas phase, as well as in chloroform, DMSO and water by considering implicit solvent (polarizable continuum model - PCM). A systematic conformational exploration revealed a few potential conformations either roughly linear or folded. The most stable conformer is folded and it was considered throughout this study.

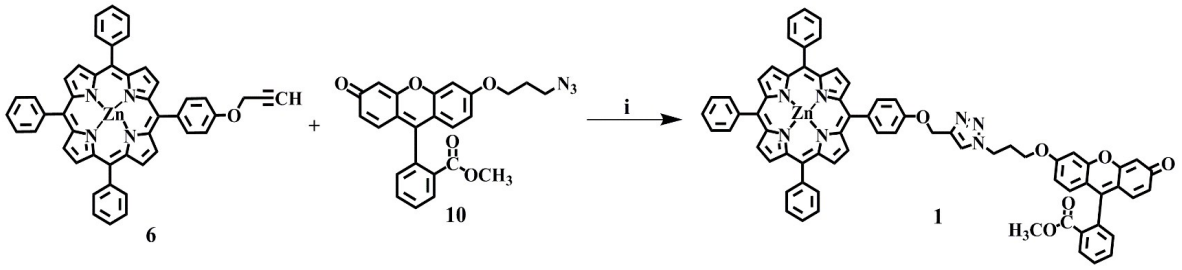

Scheme 4: Reagents and conditions: i) Copper (II) acetate, sodium ascorbate (dissolved in distillated water), THF, 24h, 91%.

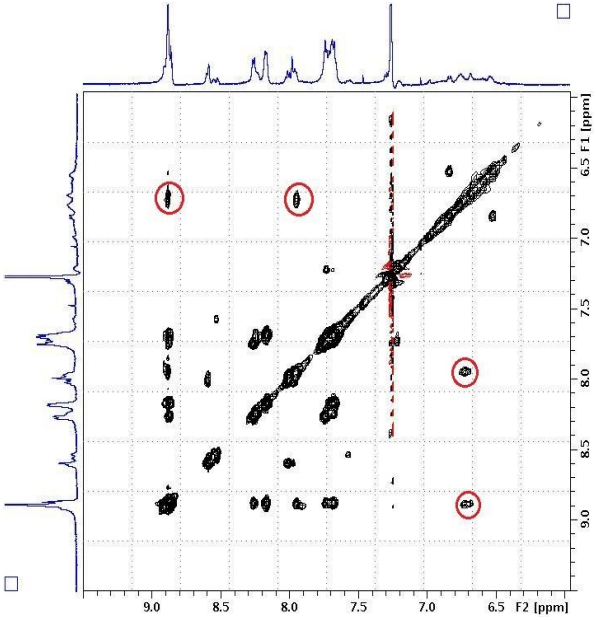

Figure 1: Aromatic region of the NOESY spectrum of **1** at 253K. The fluorescein-porphyrin correlations are circled in red.

An unfolded geometry, which corresponded to the local minimum being almost linear (Figure 2), was also considered in this study for that sake of comparison. This latter geometry avoided, as much as possible, contacts between both chromophores. All properties of both geometries were evaluated after full optimization (absence of any imaginary frequency).

The folded-type geometry is stabilized against the linear one even at the B3LYP level (relative Gibbs energy of 16.4, 75.4, 85.5 and 98.8 kJ·mol^{-1} in the gas phase, chloroform, DMSO and water, respectively in favor of the folded conformers). These results indicate significant electrostatic contributions in stabilization. At the ωB97XD level, the folded forms are additionally stabilized through dispersion interactions (*i.e.* relative Gibbs energy of 78.6, 104.7, 136.6 and 152.7 kJ·mol^{-1} in the gas phase, chloroform, DMSO and water, respectively). The folded conformer highlights in particular an attractive interaction, known as CH-π interaction,[54] between the hydrogen of the benzoate group of fluorescein and the π-system of the phenyl-substituent of porphyrin, with a distance of *ca*. 2.4 Å (lowest inter-fragment distance), as seen in Figure 2. Such interactions are known to be described by a strong dispersion contribution,[55,56] therefore requiring correct description of such interaction, as obtained with the dispersion-corrected ωB97XD functional but not with B3LYP for which the lowest distance between the two moieties is *ca*. 5.8 Å (Table 1). Solvent nature is expected to influence ratio between linear and folded form, especially promoting folded form when polarity increases. Indeed, the calculations assessed with PCM show that stabilization of the folded structure *vs*. the linear one is stronger in water (relative Gibbs energy of 152.7 kJ.mol^{-1} at the ωB97XD level, see ESI) than in chloroform (relative Gibbs energy of 104.7 kJ.mol^{-1}). Because the explicit description of solvent molecules is missing with PCM, one can imagine that the absolute values of stabilizing Gibbs energy between folded and linear forms are overestimated. Indeed in our methodology of calculation, the entropic contribution is only partially and indirectly described, and could hardly be accessible at a reasonable computational cost. This ensures a solid comparative description *i.e.*, accuracy of the relative Gibbs energies, but it possibly produces inaccurate absolute energy values. This may explain why the calculations perfectly agree with the NOESY experiments at low-temperature, but not high-temperature. When increasing temperature, the entropic contributions become most probably crucial, which should rationalize fast exchanges between conformers suggested from experimental evidences. To stress the effect of folding on optical properties, a folded and a linear conformers were considered for the theoretical analysis.

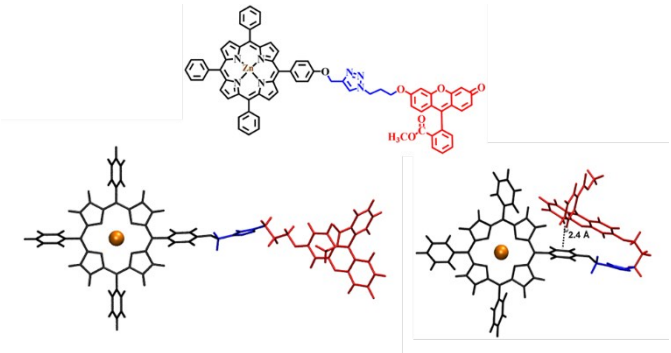

Figure 2: Structure and conformational analysis of dyad **1** (linear and folded form) with ωB97XD functional.

UV-Vis absorption properties

The UV-Vis absorption spectra of **1** and of the two reference compounds **2** and **3** performed in chloroform at 298K are shown in Figure 3, and selected data are collected in Table 2.

The UV-Vis spectrum of the porphyrin **2** is characteristic of metallated porphyrins, *i.e.*, with an intense Soret band (424 nm) and the Q-band at lower energy with vibrational structure (two peaks observed at 552 and 595 nm). This is well described by Gouterman's 'four orbital model',[48,57] which bases the analysis on transitions between HOMO (highest occupied molecular orbital, H) and H-1 to LUMO (lowest unoccupied molecular orbital, L) and L+1 (Figure 4). Similar molecular orbital (MO) schemes were obtained with both functionals (Figures 4 and 5 for B3LYP and ωB97XD, respectively), confirming the classical 'four orbital model'. As extensively described in literature, the Q-band of the metallated porphyrins corresponds to a degenerated excited state (ES); *i.e.* singlet transitions to S_1, S_2.[58] As expected, the presence of the propyloxy group slightly breaks the MO symmetry but not sufficiently to significantly break degeneracy (Figures 4 and 5).

Table 1: Distances between the two different patterns (porphyrin and fluorescein) into dyad **1**.

	B3LYP		ωB97XD	
	Lowest inter-fragment distance (Å)	Center to center (Å)*	Lowest inter-fragment distance (Å)	Center to center (Å)*
Linear form	9.5	21.13	10.8	21.15
Folded form	5.8	10.2	2.4	8.4

*Distance between the center of the metal of porphyrin moiety and the center of the xanthen-3-one moiety.

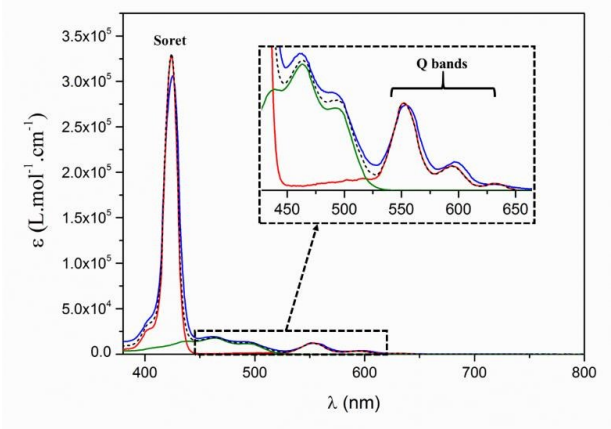

Figure 3: UV-Vis absorption spectra of dyad **1** (blue line) and of compounds **2** (red line) and **3** (green line) in $CHCl_3$ at 298 K (conc. = 2 x10^{-6} M) and mathematical sum of the two references compounds spectra (dashed line).

The fluorescein derivative **3** exhibits the typical absorption features of fluorescein. The absorption peaks at 439, 463 and 492 nm were assigned to apparent vibronic sub-bands of the first ES[59] which is mainly described by the H→L electronic transition, as seen with both functionals. Both H and L are fully delocalized over the entire xanthen-3-one moiety. Thus, almost no modification were observed compare to fluorescein, the chemical modifications being not involved in the π-conjugated system, hence not affecting π→π* electronic transitions. The experimental UV-Vis absorption spectrum of **1** matches the profile obtained by the superimposition of both spectra of **2** and **3** (Figure 3), indicating the absence of any significant interaction in the ground state. Anyway, the theoretical analysis is somewhat complex arising from the question of possible charge-transfer (CT) contributions within the ES manifold. The time dependent (TD)-DFT analysis will depend on the dyad conformation (linear *vs.* folded) and on the inclusion of long range interactions in the DFT functional (*i.e.* B3LYP *vs.* ωB97XD); in fact, although the standard functional B3LYP is widely used to evaluate optical and electronic properties of derivatives of porphyrins,[60–62] it is known to poorly described CT ES.[63] For the most stable, folded geometry of dyad **1**, B3LYP suggests a CT state of very low oscillator strength (0.01) to be the lowest ES ($S_0 \rightarrow S_1$), being somewhat below (14 nm) the Q-band formed by S_2, S_3, and essentially described by a H→L excitation (see Figure 4 and ESI). The reason for the low lying CT state is readily seen in the MO correlation diagram, see Figure 4. The energy of L is 0.53 eV below that of **2**, so that after formation of **1** (where the frontier MOs of fluorescein become destabilized) L is still formed by the fluorescein moiety. Conversely H is entirely located on the porphyrin moiety. The $S_0 \rightarrow S_4$ transition again exhibits (complex) CT character (Figure 4). In the linear conformation the low-lying CT state is absent due to the large spatial separation between the moieties. In order to decide whether CT contributions are present in the folded dyad, we performed ωB97XD and CAM-B3LYP calculations since those long-range separated XC functionals are known to better behave at describing CT states; only the ωB97XD results are shown here (Figure 5), as CAM-B3LYP provides similar results (see ESI). Different to B3LYP, no intramolecular ICT character was observed in any ES. The first two, nearly degenerated transitions to S_1, S_2 were assigned to the Q-bands of the porphyrin moiety, as described by the Gouterman's 'four orbital model'. The absence of the low lying CT state is due to the small energy difference between L of **3** and L of **2** of only 0.19 eV, which leads to greater mixing of MOs of both fragments.

Table 2: Selected photophysical data for dyad **1** and reference compounds **2** and **3** in chloroform and DMSO (298K).

	Absorption				Emission						
	Chloroform (4.81) [a]		DMSO (46.7) [a]		Chloroform (4.81) [a]			DMSO (46.7) [a]			
	λ_{abs} (nm)	ε_{abs} [b] (L.mol^{-1}.cm^{-1})	λ_{abs} (nm)	ε_{abs} [b] (L.mol^{-1}.cm^{-1})	λ_{em} (nm)	Φ_f [c,d]	τ_f λ_{obs} = 520 nm	τ_f λ_{obs} = 650 nm	λ_{em} (nm)	Φ_f [c,e]	τ_f λ_{obs} = 520 nm	τ_f λ_{obs} = 650 nm
1	427 463 492 556 598	310 000 19 000 14 000 12 000 4 500	429 460 491 562 601	402 000 17 600 11 700 12 500 6 300	530 564 604 648	0.04	2 ns (93%)[e] 450 ps (7%)[e]	1.7ns	532 564 608 662	0.07	- [e]	1,8 ns
2	424 552 595	325 000 12 000 3 000	Poorly soluble		602 654	0.05		1.6ns	Poorly soluble			
3	439 463 492	14 000 17 700 11 500	435 460 490	21 000 25 000 16 300	531 564	0.17	2.8ns		532 562	0.18	- [e]	

[a] Dielectric constant.
[b] Values represent the mean ± 8% obtained from 3 to 5 independent experiments.
[c] Using tetraphenylporphyrin (Φ_f = 0.11 in toluene), λ_{exc} = 555nm,[48] or fluoresceine (Φ_f = 0.92 in NaOH 0.1M), λ_{exc} = 490 nm as standard.[49,50]
[d] Values represent the mean ± 0.01 obtained from 3 independent experiments.
[e] Contribution percentage in the lifetime of each exponential decay.
[f] Not determined

View Article Online
DOI: 10.1039/C5NJ02901E

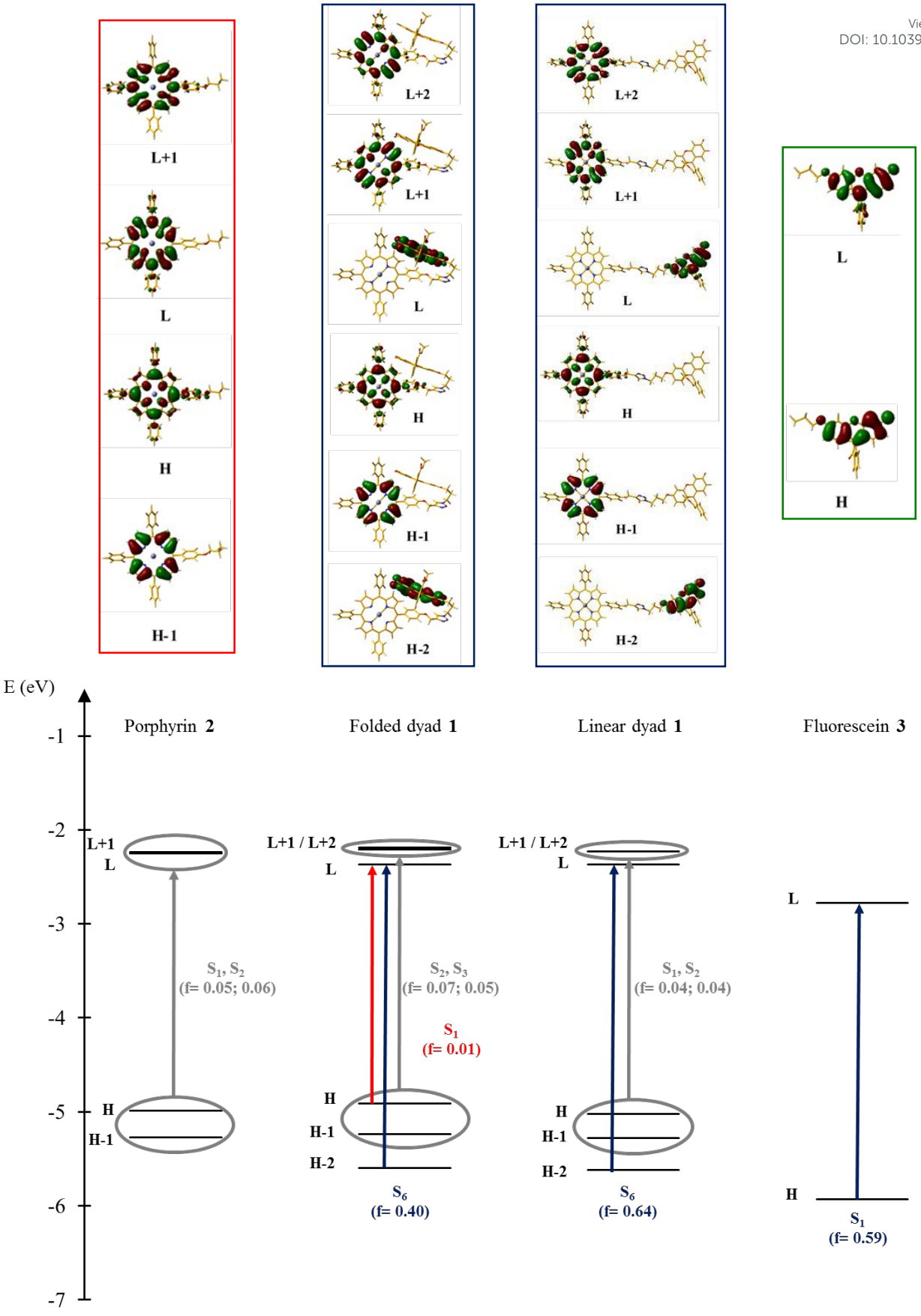

Figure 4: MO diagram of dyad **1** (folded and linear form) and reference compounds **2** and **3** using B3LYP functional.

View Article Online
DOI: 10.1039/C5NJ02901E

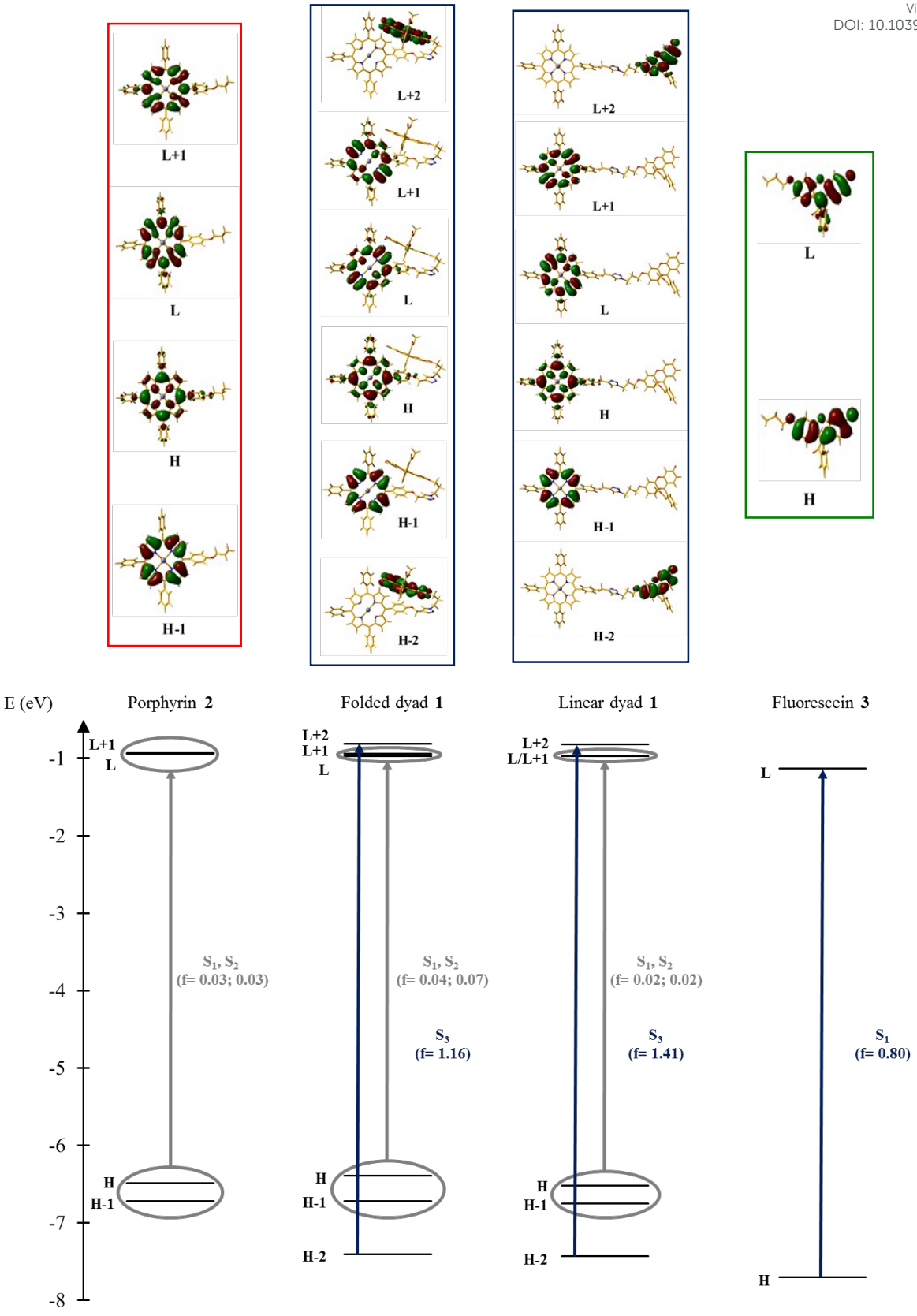

Figure 5: MO diagram of dyad **1** (folded and linear form) and reference compounds **2** and **3** using ωB97XD functional.

So that after formation of **1** the L (LUMO) is that of porphyrin (Figure 5), conversely to what was observed with B3LYP. The different behavior observed with both functionals most probably reflects the trend of B3LYP to overestimate π-delocalization, therefore over-stabilizing MO energy levels (*e.g.* here fluorescein), which may artificially generate CT states. This is also the main reason that CT contributions are negligible in the higher ES, being essentially described by mixtures of fluorescein- and porphyrin-based electronic transitions. In the linear arrangement, the occurrence of CT states becomes even more unlikely due to the spatial separation between the moieties, which is in fact reproduced by the ωB97XD calculations, see Figure 5 and ESI.

To tackle the question of CT contributions in the Q-band of **1** from the experimental side, a solvatochromic study (THF, DMF and DMSO) was conducted with **1** as well as with the two reference compounds **2** and **3**, for comparison (only results in DMSO shown, Table 2); however, the solvent polarity range was limited by the solubility of **1** and even more for **2** which is poorly soluble even in DMSO. In fact, only slight bathochromic shifts were observed from chloroform to DMSO for **1**, very similar to those for **2** and **3**. Moreover, no significant broadening of the UV-Vis spectrum was observed compared to the excitation spectrum, which would have been the case if CT state was underneath (see ESI). Thus, no evidence of the occurrence of an ICT band was found. This confirms the lack of CT contributions as suggested by the ωB97XD functional. In summary, both experimental and theoretical results revealed negligible CT contributions in the ES manifold even in the folded conformer. This agrees with the rather large center-to-center distances between the moieties of about 8-10 Å, as well as the non-parallel arrangements between the π-conjugated chromophores observed in the folded conformer; in the linear conformer, the distance is as large as 21 Å (Table 1).

Fluorescence properties

The steady-state fluorescence spectra of **1**, **2** and **3** were measured in chloroform; see Figure 6 and selected data in Table 2. After excitation at 555 nm where only the porphyrin moiety absorbs, compound **1** exhibits the same emission spectrum than the reference compound **2** (Figure 6A) as well as the same fluorescence quantum yield (Table 2). Excitation of **1** at λ_{ex} = 490 nm, *i.e.* in a region where mainly the fluorescein moiety absorbs, emissions of both fluorescein and porphyrin are seen (Figure 6A).

Conversely, preparing equimolar mixture of **2** and **3**, porphyrin emission is negligible against that of fluorescein (see Figure 6B). The dual emission of **1** contains two contributions, *i.e.* the prompt emission of the fluorescein and porphyrin moieties due to the absorbance (E) at λ_{ex} as well as (Förster-type) energy transfer (ET) as enabled by the spectral overlap between the donor (D; fluorescein) emission and the acceptor (A; porphyrin) absorption.

To calculate the efficiency of ET (Φ_{ET}), equation (1a) can be used in the absence of acceptor absorbance:[64]

$$\Phi_{ET} = \left(1 + \frac{\Phi_A}{\Phi_D} \cdot \frac{I_D}{I_A}\right)^{-1} \quad (1a)$$

where Φ_D and Φ_A are the fluorescence quantum yields of D and A, respectively; and I_D/I_A is the relative fluorescence intensity of D and A in the dyad.

In the case of acceptor absorbance, by taking the prompt fluorescence $I_{P,A}$ of the acceptor into account, Φ_{ET} is calculated by equation (1b):

$$\Phi_{ET} = \left(1 + \frac{\Phi_A}{\Phi_D} \cdot \frac{I_D}{I_A - I_{P,A}}\right)^{-1} \quad (1b)$$

where

$$I_{P,A} = I_D \cdot \frac{\Phi_A}{\Phi_D} \cdot \frac{A_A}{A_D} \quad (2)$$

With $A=1-10^{-E}$.

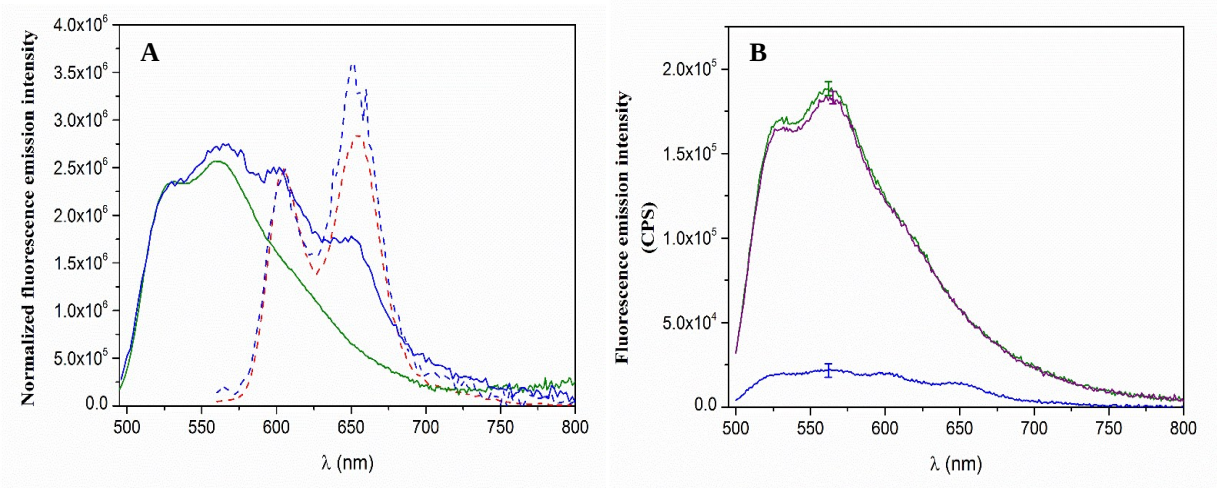

Figure 6: Fluorescence emission spectra of dyad **1** (blue line), reference compound **2** (red line), reference compound **3** (green line) and an equimolar mixture of compounds **2** and **3** (purple line). All experiments were performed in $CHCl_3$, at 298K and with a concentration at ca. 10^{-6}M.

6A: Normalized fluorescence emission spectra at λ_{exc} = 555 nm (dashed lines) and at λ_{exc} = 490 nm (solid lines).

6B: Emission spectra at λ_{exc} = 490 nm. Emission maxima values represent the mean ± 2% obtained from 3 independent experiments.

This leads to:

$$\Phi_{ET} = \left(1 + \frac{\Phi_A}{\Phi_D} \cdot \frac{1}{I_A / I_D - (\Phi_A / \Phi_D) \cdot (A_A / A_D)}\right)^{-1} \quad (1c)$$

Inserting the values in chloroform from Table 2, a Φ_{ET} value of 0.42 ± 0.08 (average from two measurements) is calculated.

The transfer efficiency is also accessible from time-resolved measurements (3):

$$\Phi_{ET} = 1 - \tau_{D,A} / \tau_D \quad (3)$$

where τ_D and $\tau_{D,A}$ are the fluorescence lifetimes of the donor molecule and of dyad **1** upon excitation of the donor moiety (520 nm), respectively. Using the values of Table 2, the Φ_{ET} equals 0.33, being relatively close to the steady state value. It should be mentioned that the fluorescence decay of the dyad is somewhat non-exponential (Table 2), which might reflect the complex excited state relaxation in the dyad, as observed for other flexible systems.[65] On the other hand, the direct excitation of the acceptor unit (porphyrin *i.e.* 650 nm) provided, as expected a very similar value ($\tau_{A,D}$ = 1.9 ns) as compared to that of the free porphyrin **2** (τ_A = 1.7 ns), see Table 2.

In order to investigate the effect of solvent polarity on energy transfer efficiency, the same study was conducted in DMSO (Figure 2 in ESI). No shift of the emission maxima was observed (Table 2). Interestingly, Φ_{ET}, is dramatically increased from chloroform to DMSO, where it equals 0.75 using equation (1b). We tentatively assigned the increase of ET in DMSO to the formation of non-covalent dimers or n-mers due to decreased solubility in the polar solvent. This might indeed bring the donor and acceptor moieties in closer contact by intermolecular interaction (mainly π-π stacking between fluorescein and porphyrin) and thus enhance ET.

Conclusions

In this article, a novel fluorescein-Zn-porphyrin dyad built with a triazole linkage was studied both experimentally and theoretically. According to NOESY analysis, a folding conformer is likely to exist, which has been confirmed by conformational analysis of the dyad. Non-covalent interactions including electrostatic and CH-π interaction strongly stabilized folded with respect to unfolded geometries. Fluorescence spectroscopy has revealed an intramolecular energy transfer between the two patterns (fluorescein and porphyrin), which has appeared more efficient in DMSO than in chloroform as expected. Further investigations such as fast time-resolved spectroscopy should provide further insight into the interaction between the porphyrin and fluorescein moieties. Likewise, synthesis and study of fluorescein tagged porphyrins with linkers more or less flexible are currently in progress in our laboratory. This study has paved the way towards an optimal use of tagged-porphyrins in plant cells to understand mechanisms of the herbicide action. In this context, water solubilization has been envisaged through vectorization.

Experimental

View Article Online
DOI: 10.1039/C5NJ02901E

Materials

All organic materials were purchased from commercial suppliers (Acros Organics, Alfa Aesar, Sigma-Aldrich or TCI) and used as received. Solvents used in the UV-Vis and fluorescence measurements were of spectroscopic quality and they were stored in a dark place. Analytical thin layer chromatography (TLC) was performed on Merck 60F254 silica gel. Merck precoated plates (silica gel 60, 2 mm) were used for preparative thin layer chromatography. Column chromatography was carried out with silica gel (60 ACC, 15-40 µm, Merck).

Instrumentation

^{1}H and ^{13}C nuclear magnetic resonance (^{1}H-NMR and ^{13}C-NMR) spectra were recorded in $CDCl_3$, on Bruker DPX 400 and 500 spectrometers. ^{1}H and NOESY spectra at variable temperature were recorded in $CDCl_3$, on a Bruker DRX 500 spectrometer with a BVT3000 variable temperature unit. Chemical shifts are reported as δ (parts per million), downfield from internal TMS. IR spectra were performed with a Perkin Elmer Spectrum 1000 photometer, with samples conditioned on KBr pellets. Melting points (Mp) were uncorrected.

Mass spectra were performed with a 4800 MALDI TOF/TOF™ Analyzer from AB SCIEX for all porphyrins derivatives and dyad **1**. For fluorescein derivatives, high resolution electrospray ionization mass spectra (HR ESI-MS) were performed on a Bruker maXis mass spectrometer by the ICOA/CBM (FR2708) platform.

Ultraviolet-visible spectra (UV-Vis) and fluorescence spectra were recorded using 10 mm quartz cells. UV-Vis were recorded on a SPECORD® 210 double beam spectrophotometer using 10 mm quartz cells.

Steady-state photoluminescence spectra were recorded using a FLS980 spectrometer (Edinburgh Instruments, UK equipped with a 450 W xenon lamp. Detection was made in the 300–800 nm range using a cooled R928P Hamamatsu photomultiplier (dark count 50 cps). Quantum yields were measured using tetraphenylporphyrin (H_2TPP)[66] in toluene and commercial fluorescein (spectroscopic quality)[67,68] in aqueous NaOH 0.1M as standards.

Time-resolved spectroscopy measurements were performed on the same apparatus, using time correlated single photon counting (TCSPC) and a picosecond diode laser at 509.2 nm as excitation source (temporal width of 150 ps). The instrument response function was measured using a diffusive reference sample (LUDOX ® from Sigma-Aldrich).

Synthesis

***5-(4-hydroxyphenyl)-10,15,20-triphenylporphyrin* (4).** 4-hydroxy-benzaldehyde (1 equiv., 1.22 g, 10 mmol) and benzaldehyde (3 equiv., 3.1 mL, 30 mmol) were dissolved in 200 mL of propionic acid. The solution was heated at 120°C under reflux with vigorous stirring

View Article Online
DOI: 10.1039/C5NJ02901F

for 1h, then freshly distilled pyrrole (4 equiv., 2.8 mL, 40 mmol) were added. After 1 h, the mixture was cooled and the solvent was evaporated to dryness and the crude product was purified by column (silica gel, petroleum ether with $CHCl_3$ gradient ranging from 70 to 100%). Compound **4** was obtained as a purple solid (435 mg, 7%).
^{1}H NMR ($CDCl_3$, 400 MHz) δ_{ppm}: 8.87 (d, 2H, J=4.8Hz); 8.83 (s_{el}, 6H); 8.21 (d, 6H, J=7.6 Hz); 8.04 (d, 2H, J=8.3 Hz); 7.75 (d, 9H, 7.4 Hz); 7.16 (d, 2H, J=8.2 Hz); -2.74 (s, 2H).
^{13}C NMR ($CDCl_3$, 400 MHz) δ_{ppm}: 155.4; 142.2; 135.7; 134.8; 134.6; 133.9; 132.3: 131.9; 131.2; 131.0; 130.9; 129.0; 128.6; 128.5; 128.3; 128.0; 127.8; 126.7; 120.1; 120.0; 119.7; 113.7.
MS (MALDI-TOF): m/z = 631.52 $[M+H]^+$.
UV-Vis ($CHCl_3$) λ_{max} nm (ε, 10^{-3} L.mol^{-1}.cm^{-1}): 419 (563), 518 (11), 556 (9), 598 (3), 647 (1).

5-(4-propargyloxyphenyl)-10,15,20-triphenylporphyrin (5). 5-(4-hydroxyphenyl)-10,15,20-triphénylporphyrine **4** (1 equiv., 140 mg, 0.22 mmol), propargyl bromide (20 equiv., 0.93 mL, 4.4 mmol), K_2CO_3 (20 equiv., 605 mg, 4.4 mmol) were dissolved in dry DMF (30 mL). The solution was stirred in the dark for 24h under argon and at room temperature. After solvent removing, the crude product was dissolved in DCM, washed with distillated water (2x25 mL) and dried over $MgSO_4$. The residue was purified by column (silica gel, $CHCl_3$) to give compound **5** as a purple solid (116 mg, 79%).
^{1}H NMR ($CDCl_3$, 400 MHz) δ_{ppm}: 8.87 (d, 2H, J=4.8Hz); 8.83 (s_{el}, 6H); 8.21 (d, 6H, J=7.6 Hz); 8.04 (d, 2H, J=8.3 Hz); 7.75 (d, 9H, 7.4 Hz); 7.16 (d, 2H, J=8.2 Hz); 4.98 (d, 2H, J=2.3 Hz); 2.69 (t, 1H, J=2.3 Hz); -2.74 (s, 2H).
^{13}C NMR ($CDCl_3$, 400 MHz) δ_{ppm}: 157.4; 139.3; 137.3; 135.6; 135.5; 134.5; 133.8; 132.1; 131.0; 129.3; 128.7; 127.4; 120.1; 119.4; 113.1; 78.7; 76.8; 56.2.
MS (MALDI-TOF): m/z = 669.23 $[M+H]^+$.
UV-Vis ($CHCl_3$) λ_{max} nm (ε, 10^{-3} L.mol^{-1}.cm^{-1}): 419 (337), 518 (13), 556 (6), 598 (3), 647 (1).
IR υ (cm^{-1}), KBr: 2118 (C≡C) ; 3282 (C-H).

Zinc(II) 5-(4-propargyloxyphenyl)-10,15,20-triphénylporphyrin (6). 5-(4-propargyloxyphényl)-10,15,20-triphénylporphyrine **5** (1 equiv., 115.8 mg, 0.17 mmol) and zinc (II) acetate (10 equiv., 311 mg, 1.7 mmol) were dissolved in a solution of $CHCl_3$/MeOH (1/1, v/v). The mixture was stirred during one night at room temperature. After solvent evaporation, the product was dissolved in DCM and washed with distillated water (2x25 mL), then dried over $MgSO_4$ to give compound **6** (123.5 mg, >99%).
^{1}H NMR ($CDCl_3$, 400 MHz) δ_{ppm}: 8.88 (d, 2H, J=4.7Hz); 8.84 (s_{el}, 6H); 8.21 (d, 6H, J=7.4 Hz); 8.14 (d, 2H, J=8.4 Hz); 7.75 (d, 9H, 7.4 Hz); 7.36 (d, 2H, J=8.5 Hz); 4.99 (d, 2H, J=2.4 Hz); 2.69 (t, 1H, J=2.3 Hz).
^{13}C NMR ($CDCl_3$, 400 MHz) δ_{ppm}: 157.4; 139.3; 137.3; 135.6; 135.5; 134.5; 133.8; 132.1; 131.0; 129.3; 128.7; 127.4; 120.1; 119.4; 113.1; 78.7; 76.8; 56.2.
MS (MALDI-TOF): m/z = 731.15 $[M+H]^+$.
UV-Vis ($CHCl_3$) λ_{max} nm (ε, 10^{-3} L.mol^{-1}.cm^{-1}): 426 (301), 556 (12), 598 (3.7).
IR υ (cm^{-1}), KBr: 2118 (C≡C); 3282 (C-H).

5-(4-propoxyphenyl)-10,15,20-triphenylporphyrin (7). Compound **4** (1 equiv., 59 mg, 0.09 mmol), 1-bromopropane (5 equiv., 41 µL, 0.45 mmol) and K_2CO_3 (10 equiv., 124.4 mg, 0.9 mmol) were dissolved in dry DMF (10 mL). The reaction was activated twice by micro-waves irradiations (5'/ 200 W/ 120°C). After solvent evaporation, the crude product was dissolved in DCM, washed with distillated water (2x25 mL) then dried over $MgSO_4$. The residue was purified on column (silica gel, $CHCl_3$) to give compound **7** as a purple solid (47.3 mg, 78%).
^{1}H NMR ($CDCl_3$, 400 MHz) δ_{ppm}: 8.87 (d, 2H, J=4.8Hz); 8.83 (s_{el}, 6H); 8.21 (d, 6H, J=7.6 Hz); 8.04 (d, 2H, J=8.3 Hz); 7.75 (d, 9H, 7.4 Hz); 7.16 (d, 2H, J=8.2 Hz); 4.32 (t, 2H, J=6.8 Hz); 1.84 (m, 2H); 1.04 (t, 3H, J=7.3 Hz); -2.74 (s, 2H).
^{13}C NMR ($CDCl_3$, 400 MHz) δ_{ppm}: 157.5; 139.3; 137.3; 135.6; 135.5; 134.5;133.9; 133.8; 132.3; 132.1; 131.0; 129.3; 128.7; 127.4; 120.1; 119.4; 113.7; 69.1; 23.8; 12.5.
MS (MALDI-TOF): m/z = 673.32 $[M+H]^+$.
UV-Vis ($CHCl_3$) λ_{max} nm (ε, 10^{-3} L.mol^{-1}.cm^{-1}): 418 (342), 518 (16), 552 (12), 595 (3), 648 (1).

Zinc(II) 5-(4-propoxyphenyl)-10,15,20-triphenylporphyrin (2). Compound **7** (1 equiv., 26.1 mg, 0.04 mmol) and zinc (II) acetate (10 equiv., 85.6 mg, 0.4 mmol) were dissolved in a solution of $CHCl_3$/MeOH (1/1, v/v). The mixture was stirred during one night at room temperature. After solvent evaporation, the product was dissolved in DCM and washed with distillated water (2x15 mL), then dried over $MgSO_4$ to give compound **2** as a purple solid (26.7 mg, >99%).
^{1}H NMR ($CDCl_3$, 400 MHz) δ_{ppm}: 8.87 (d, 2H, J=4.8Hz); 8.83 (s_{el}, 6H); 8.21 (d, 6H, J=7.6 Hz); 8.04 (d, 2H, J=8.3 Hz); 7.75 (d, 9H, 7.4 Hz); 7.16 (d, 2H, J=8.2 Hz); 4.32 (t, 2H, J=6.8 Hz); 1.84 (m, 2H); 1.04 (t, 3H, J=7.3 Hz).
^{13}C NMR ($CDCl_3$, 400 MHz) δ_{ppm}: 157.5; 139.3; 137.3; 135.6; 135.5; 134.5;133.9; 133.8; 132.3; 132.1; 131.0; 129.3; 128.7; 127.4; 120.1; 119.4; 113.7; 69.1; 23.8; 12.5.
MS (MALDI-TOF): m/z = 735.24 $[M+H]^+$.
UV-Vis ($CHCl_3$) λ_{max} nm (ε, 10^{-3} L.mol^{-1}.cm^{-1}): 424 (290), 552 (12), 595 (3).

Methyl 2-(6-hydroxy-3-oxo-3H-xanthen-9-yl)benzoate (8). Fluorescein (1 equiv., 2.76g, 8.3 mmol) was dissolved in freshly distillated MeOH (200 mL). Fuming sufuric acid (1 mL) was added dropwise, then the mixture was stirring in the dark for 18h. The reaction was stopped by addition of cooled water, then the solution was filtered to give compound **8** as an orange solid (2.8 g, 98 %).
Tf : 228°C.
^{1}H NMR ($CDCl_3$, 400 MHz) δ_{ppm}: 8.25 (dd, 1H, ^{3}J=7.8 Hz, ^{4}J=1.2 Hz); 7.74 (dt, 1H, ^{3}J=7.5 Hz, ^{4}J=1.4 Hz); 7.66 (dt, 1H, ^{3}J=7.6 Hz, ^{4}J=1.4 Hz); 7.30 (dd, 1H, ^{3}J=7.5 Hz, ^{4}J=1 Hz); 6.96 (d, 1H, J=2.4 Hz); 6.89 (d, 1H, J=8.8 Hz); 6.85 (d, 1H, J=9.7 Hz); 6.74 (dd, 1H, ^{3}J=8.9 Hz, ^{4}J=2.4 Hz); 6.55 (dd, 1H, ^{3}J=9.7 Hz, ^{4}J=1.7 Hz); 6.47 (d, 1H, J=1.6 Hz); 3.64 (s, 3H).
^{13}C NMR ($CDCl_3$, 400 MHz) δ_{ppm}: 185.7; 165.6; 159.0; 154.4 (2C); 149.2; 134.7 (2C); 132.7; 130.4 (2C); 130.2; 129.6 (2C); 128.8; 117.5; 105.7 (2C); 100.8 (2C); 52.4 (O-$\underline{C}H_3$).
HRMS (ESI-Q3): m/z = 347.09 $[M+H]^+$.
UV-Vis ($CHCl_3$) λ_{max} nm (ε, 10^{-3} L.mol^{-1}.cm^{-1}) : 438 (12), 462 (15), 491 (10).

Methyl 2-(6-(3-bromopropoxy)-3-oxo-3H-xanthen-9-yl)benzoate (9). Methyl 2-(6-hydroxy-3-oxo-3H-xanthen-9-yl)benzoate **8** (1

View Article Online DOI: 10.1039/C5NJ02901E

equiv., 330 mg, 0.95 mmol), 1,3-dibromopropane (3 equiv., 290 µL, 2.85 mmol) and K_2CO_3 (10 equiv., 1.3 g, 9.5 mmol) were dissolved in dry DMF (25 mL). The solution was stirring at room temperature, in the dark and under argon for 20h. After solvent evaporation, the residue was dissolved in $CHCl_3$ and washed with distillated water (3x25 mL). Then the crude product was purified by column (silica gel, $CHCl_3$) to give compound **5** as an orange oil (285.7 mg, 64%).

^{1}H NMR ($CDCl_3$, 400 MHz) δ_{ppm}: 8.25 (dd, 1H, ^{3}J=7.8 Hz, ^{4}J=1.2 Hz); 7.74 (dt, 1H, ^{3}J=7.5 Hz, ^{4}J=1.4 Hz); 7.66 (dt, 1H, ^{3}J=7.6 Hz, ^{4}J=1.4 Hz); 7.30 (dd, 1H, ^{3}J=7.5 Hz, ^{4}J=1 Hz); 6.96 (d, 1H, J=2.4 Hz); 6.89 (d, 1H, J=8.8 Hz); 6.85 (d, 1H, J=9.7 Hz); 6.74 (dd, 1H, ^{3}J=8.9 Hz, ^{4}J=2.4 Hz); 6.55 (dd, 1H, ^{3}J=9.7 Hz, ^{4}J=1.7 Hz); 6.47 (d, 1H, J=1.6 Hz); 4.24 (t, 2H, J=5.8 Hz); 3.64 (s, 3H); 3.60 (t, 2H, J=6.3 Hz); 2.37 (quint, 2H, J=6.06 Hz).

^{13}C NMR ($CDCl_3$, 400 MHz) δ_{ppm}: 185.8; 165.6; 163.7; 159.0; 154.3; 150.1; 134.7; 132.6; 131.1; 130.6; 130.4; 130.2; 129.9; 129.6; 128.8; 117.5; 114.7; 113.8; 105.8; 100.8; 70.4; 52.4; 33.9; 27.3.

HRMS (ESI-Q3): m/z = 467.09 $[M+H]^+$.

UV-Vis ($CHCl_3$) λ_{max} nm (ε, 10^{-3} L.mol^{-1}.cm^{-1}) : 438 (12), 461 (16), 491 (10).

Methyl 2-(6-(3-azidopropoxy)-3-oxo-3H-xanthen-9-yl)benzoate (10). Methyl 2-(6-(3-bromopropoxy)-3-oxo-3H-xanthen-9-yl) benzoate **9** (1 equiv., 286 mg, 0.61 mmol) and sodium azide (4 equiv., 158.6 mg, 2.44 mmol) were dissolved in dry DMF (15 mL). The solution was stirring in the dark for 24h, at room temperature and under argon. After solvent evaporation, the crude product was dissolved in DCM and washed twice with distillated water (2x25 mL), then dried over $MgSO_4$ to give compound **10** as an orange oil (261.8 mg, >99%).

^{1}H NMR ($CDCl_3$, 400 MHz) δ_{ppm}: 8.24 (dd, 1H, ^{3}J=7.6 Hz, ^{4}J=1.2 Hz); 7.74 (dt, 1H, ^{3}J=7.5 Hz, ^{4}J=1.3 Hz); 7.67 (dt, 1H, ^{3}J=7.6 Hz, ^{4}J=1.4 Hz); 7.30 (dd, 1H, ^{3}J=7.5 Hz, ^{4}J=1 Hz); 6.96 (d, 1H, J=2.4 Hz); 6.90 (d, 1H, J=8.9 Hz); 6.85 (d, 1H, J=9.7 Hz); 6.74 (dd, 1H, ^{3}J=8.9 Hz, ^{4}J=2.4 Hz); 6.55 (dd, 1H, ^{3}J=9.7 Hz, ^{4}J=1.5 Hz); 6.47 (d, 1H, J=1.6 Hz); 4.17 (t, 2H, J=5.7 Hz); 3.63 (s, 3H); 3.53 (t, 2H, J=6.5 Hz); 2.10 (quint, 2H, J=6.4 Hz).

^{13}C NMR ($CDCl_3$, 400 MHz) δ_{ppm}: 185.8; 165.6; 163.7; 159.0; 154.3; 150.1; 134.7; 132.6; 131.1; 130.6; 130.4; 130.2; 129.9; 129.6; 128.8; 117.5; 114.7; 113.8; 105.8; 100.8; 68.8; 52.4; 42.7; 30.4.

UV-Vis ($CHCl_3$) λ_{max} nm (ε, 10^{-3} L.mol^{-1}.cm^{-1}): 439 (11), 463 (15), 492 (9).

IR υ (cm^{-1}), KBr: 2099 (N_3).

Methyl 2-(3-oxo-6-propoxy-3H-xanthen-9-yl)benzoate (3). Compound **8** (1 equiv., 173.2 mg, 0.5 mmol), 1-bromopropane (3 equiv., 136.4 µL, 1.5 mmol) and K_2CO_3 (20 equiv., 1.38 g, 10 mmol) were dissolved in dry DMF (20 mL). The solution was stirring for 18h in the dark, at room temperature and under argon. After solvent evaporation, the residue was dissolved in DCM and washed twice with distillated water (2x25 mL), then dried over $MgSO_4$. To finish, the product was purified on column (silica gel, DCM) to give compound **3** as an orange solid (172.8 mg, 89%).

^{1}H NMR ($CDCl_3$, 400 MHz) δ_{ppm}: 8.24 (dd, 1H, ^{3}J=7.2 Hz, ^{4}J=1.2 Hz); 7.73 (dt, 1H, ^{3}J=7.4 Hz, ^{4}J=0.9 Hz); 7.66 (dt, 1H, ^{3}J=7.6 Hz, ^{4}J=0.9 Hz); 7.31 (dd, 1H, ^{3}J=7.2 Hz, ^{4}J=1 Hz); 6.94 (d, 1H, J=2.3 Hz); 6.87 (d, 1H, J=8.9 Hz); 6.84 (d, 1H, J=9.7 Hz); 6.73 (dd, 1H, ^{3}J=8.9 Hz, ^{4}J=2.3 Hz); 6.54 (dd, 1H, ^{3}J=9.7 Hz, ^{4}J=1.8 Hz); 6.45 (d, 1H, J=1.8 Hz); 4.02 (t, 2H, J=6.5 Hz); 3.63 (s, 3H); 1.86 (m, 2H); 1.06 (t, 3H, J=7.4 Hz).

^{13}C NMR ($CDCl_3$, 400 MHz) δ_{ppm}: 185.8; 165.6; 163.7; 159.0; 154.3; 150.1; 134.7; 132.6; 131.1; 130.6; 130.4; 130.2; 129.9; 129.6; 128.8; 117.5; 114.7; 113.8; 105.8; 100.8; 70.4; 52.4; 22.3; 10.4.

HRMS (ESI-Q3): m/z = 389.13 $[M+H]^+$.

UV-Vis ($CHCl_3$) λ_{max} nm (ε, 10^{-3} L.mol^{-1}.cm^{-1}) : 439 (14), 463 (17), 492 (11).

Dyad (1). Compound **6** (1 equiv., 276.7 mg, 0.38 mmol) and compound **10** (1.5 equiv., 250.8 mg, 0.57 mmol) were dissolved in THF (45 mL). Copper (II) acetate (2.7 equiv., 187 mg, 1.03 mmol) and sodium ascorbate (7 equiv., 527 mg, 2.66 mmol) preliminary dissolved in distillated water (4 mL) were added. The mixture was stirring for 24h, in the dark and at room temperature. After solvent evaporation, the crude product was dissolved in DCM and washed with distillated water (2x25 mL), then dried over $MgSO_4$. Finally residue was purified on column (silica gel, DCM with EtOH gradient ranging from 0 to 10%) to give compound **1** as a red-orange solid (403.5 mg, 91%).

^{1}H NMR ($CDCl_3$, 500 MHz)

Porphyrin moiety: δ_{ppm}: 8.86 (d, 8H, J=4.7Hz); 8.18 (d, 6H, J=7.7 Hz); 7.98 (d, 2H, J=8.3 Hz); 7.69 (m, 9H); 7.56 (d, 2H, J=8.5 Hz); 5.66 (d, 2H, J=2.4 Hz).

Fluorescein moiety : δ_{ppm}: 8.24 (dd, 1H, ^{3}J=7.5 Hz, ^{4}J=1.2 Hz); 7.72 (dt, 1H, ^{3}J=7.5 Hz, ^{4}J=1.3 Hz); 7.61 (dt, 1H, ^{3}J=7.6 Hz, ^{4}J=1.4 Hz); 7.28 (dd, 1H, ^{3}J=7.5 Hz, ^{4}J=1 Hz); 6.95 (d, 1H, J=2.4 Hz); 6.85 (d, 1H, J=8.9 Hz); 6.79 (d, 1H, J=8.9 Hz); 6.71 (dd, 1H, ^{3}J=8.9 Hz, ^{4}J=2.4 Hz); 6.61 (dd, 1H, ^{3}J=8.8 Hz, ^{4}J=2.1 Hz); 6.49 (d, 1H, J=1.6 Hz); 3.91 (t, 2H, J=5.9 Hz); 3.60 (s, 3H); 3.50 ($s_{el.}$, 2H); 2.01 (m, 2H).

Triazole moiety: δ_{ppm}: 8.14 (s,1H).

^{13}C NMR ($CDCl_3$, 500 MHz)

Porphyrin moiety : δ_{ppm}: 157.4; 136.4; 135.9; 135.8; 134.8; 134.4; 133.8; 132.6; 131.0; 129.6; 128.9; 127.3; 120.1; 113.5; 76.6.

Fluorescein moiety: δ_{ppm}: 184.6; 165.6; 162.6; 158.3; 154.0; 150.1; 134.8; 132.7; 131.1; 130.6; 130.4; 130.2; 129.8; 129.6; 128.9; 117.3; 115.0; 112.8; 105.0; 100.9; 65.4; 52.4; 47.9; 22.6.

Triazole moiety: δ_{ppm}: 143.3; 129.1.

MS (MALDI-TOF): m/z = 1160.34 $[M+H]^+$.

UV-Vis ($CHCl_3$) λ_{max} nm (ε, 10^{-3} L.mol^{-1}.cm^{-1}): 427 (310), 463 (20), 492 (13), 556 (12), 598 (4.5).

IR υ (cm^{-1}), KBr: 2102 (C-N).

Theoretical calculations

Quantum chemistry calculations based on DFT were performed to investigate the conformational space of compounds **1**, **2** and **3**. Because of the structure of **1**, non-covalent interactions between the porphyrin and fluorescein moieties were expected. In particular, a proper description of dispersive forces appeared mandatory. The use of the ωB97XD XC functional has been described to properly describe non-covalent interactions.[52,53] The robustness of ωB97XD at describing non-covalent interactions was confirmed to better describe non-covalent interactions (π-π stacking and H-bonding). The conformational analysis was assessed by a systematic exploration of the potential energy surface of the triazole linkage. The most stable conformers were confirmed by the absence of any imaginary

frequency. The Pople-type double-ζ basis set 6-31+G(d,p) was used as being an adapted compromise between accuracy and time consumption. Adding diffuse function (+) is mandatory to better evaluate electron distribution on these highly π-conjugated systems. When necessary, the extensively recommend LANL2DZ basis set, using core pseudo potentials, was used for the transition metal Zn.[69] Solvent effects were taken into account implicitly using the IEFPCM (Integral Equation Formalism Polarizable Continuum Model). In PCM models, the substrate is embedded into a shape-adapted cavity surrounded by a dielectric continuum characterized by its dielectric constant (ε = 78.35 and 4.71 in water and $CHCl_3$, respectively). Optical properties (*i.e.,* UV-Vis absorption and ES description) were predicted by using TD(Time Dependent)-DFT calculations. Three different functionals were used, namely B3LYP as classically used for porphyrins and dyads and the long-range separated functionals, namely ωB97XD and CAM-B3LYP, due to their capacity to properly describe CT in ES. Only the ωB97XD results are provided here as CAM-B3LYP similar results. All calculations were performed with Gaussian09.[70]

Photophysical properties

All solutions were prepared at a concentration about 10^{-6} M, and the masses weighed using a microbalance. Ultraviolet-visible (UV-Vis), fluorescence and time-resolved spectroscopy measurements were recorded using 10 mm quartz cells, at room temperature (detection was made in the 300–800 nm range).

Quantum yields were measured using tetraphenylporphyrin (H_2TPP)[66] in toluene and commercial fluorescein (spectroscopic quality)[67,68] in aqueous NaOH 0.1M as standards; Φ_f (H_2TPP) = 0.11, Φ_f (fluorescein) = 0.92.

Time-resolved spectroscopy measurements were performed using time correlated single photon counting (TCSPC) and a picosecond diode laser at 509.2 nm as excitation source (temporal width of 150 ps). The instrument response function was measured using a diffusive reference sample (LUDOX ® from Sigma-Aldrich).

Acknowledgements

P. Trouillas and S. Leroy-Lhez thank the French National Research Agency (ANR Porphy-Plant) for financial support. The authors thank the "Conseil Régional du Limousin" for financial support and CALI (CAlcul en LImousin) for the theoretical study. The work at IMDEA was supported by the Spanish Ministerio de Economía y Competitividad (MINECO; project MultiCrom, grant no. CTQ2014-58801). The authors also thank Dr Yves Champavier for all NMR analysis, Mr Cyril Colas from ICOA for all mass spectra and to finish the joint service PLATINOM (XLIM Research Institute / CNRS 7252). P. Trouillas thanks the Czech Science Foundation (P208/12/G016), the Ministry of Education, Youth and Sports of the Czech Republic (project LO1305) and the Operational Program Education for Competitiveness-European Social Fund (project CZ.1.07/2.3.00/20.0058 of the Ministry of Education, Youth and Sports of the Czech Republic) is also gratefully acknowledged.

Notes and references

1 D. Mauzerall, in *Photosynthesis I*, eds. P. D. A. Trebst and P. D. M. Avron, Springer Berlin Heidelberg, 1977, pp. 117–124.
2 H. L. Bonkovsky, J.-T. Guo, W. Hou, T. Li, T. Narang and M. Thapar, in *Comprehensive Physiology*, John Wiley & Sons, Inc., 2013.
3 M. Biesaga, K. Pyrzyńska and M. Trojanowicz, *Talanta*, 2000, **51**, 209–224.
4 L.-L. Li and E. W.-G. Diau, *Chem. Soc. Rev.*, 2013, **42**, 291–304.
5 M.-E. Ragoussi and T. Torres, *Chem. Commun.*, 2015, **51**, 3957–3972.
6 R. A. Sheldon, *Metalloporphyrins in Catalytic Oxidations*, CRC Press, 1994.
7 J. D. Spikes and G. Jori, *Lasers Med. Sci.*, 1987, **2**, 3–15.
8 I. Stojiljkovic, B. D. Evavold and V. Kumar, *Expert Opin. Investig. Drugs*, 2001, **10**, 309–320.
9 M. Ethirajan, Y. Chen, P. Joshi and R. K. Pandey, *Chem. Soc. Rev.*, 2011, **40**, 340–362.
10 C. A. Rebeiz, K. N. Reddy, U. B. Nandihalli and J. Velu, *Photochem. Photobiol.*, 1990, **52**, 1099–1117.
11 C. Riou, C. A. Calliste, A. Da Silva, D. Guillaumot, O. Rezazgui, V. Sol and S. Leroy-Lhez, *Photochem. Photobiol.*, 2014, **13**, 621–625.
12 C. A. Rebeiz, L. J. Gut, K. Lee, J. A. Juvik, C. C. Rebeiz, C. E. Bouton and D. G. H. N. Towers, *Crit. Rev. Plant Sci.*, 1995, **14**, 329–366.
13 T. Ben Amor and G. Jori, *Insect Biochem. Mol. Biol.*, 2000, **30**, 915–925.
14 C. Fabris, M. Soncin, G. Jori, A. Habluetzel, L. Lucantoni, S. Sawadogo, L. Guidolin and O. Coppellotti, *Photochem. Photobiol. Sci.*, 2012, **11**, 294–301.
15 S. Campidelli, R. Deschenaux, A. Swartz, G. M. A. Rahman, D. M. Guldi, D. Milic, E. Vázquez and M. Prato, *Photochem. Photobiol.*, 2006, **5**, 1137–1141.
16 S. Punidha, J. Sinha, A. Kumar and M. Ravikanth, *J. Org. Chem.*, 2008, **73**, 323–326.
17 Y. Pareek and M. Ravikanth, *Tetrahedron*, 2013, **69**, 1590–1599.
18 V. Nikolaou, K. Karikis, Y. Farré, G. Charalambidis, F. Odobel and A. G. Coutsolelos, *Dalton Trans.*, 2015, **44**, 13473–13479.
19 M. K. Panda, K. Ladomenou and A. G. Coutsolelos, *Coord. Chem. Rev.*, 2012, **256**, 2601–2627.
20 H. Imahori and S. Fukuzumi, *Adv. Funct. Mater.*, 2004, **14**, 525–536.
21 M. G. Walter, A. B. Rudine and C. C. Wamser, *J. Porphyrins Phthalocyanines*, 2010, **14**, 759–792.
22 M. Urbani, M. Grätzel, M. K. Nazeeruddin and T. Torres, *Chem. Rev.*, 2014, **114**, 12330–12396.
23 A. Yella, C.-L. Mai, S. M. Zakeeruddin, S.-N. Chang, C.-H. Hsieh, C.-Y. Yeh and M. Grätzel, *Angew. Chem. Int. Ed. Engl.*, 2014, **53**, 2973–2977.
24 N. Zhang, B. Zhang, J. Yan, X. Xue, X. Peng, Y. Li, Y. Yang, C. Ju, C. Fan and Y. Feng, *Renew. Energy*, 2015, **77**, 579–585.
25 B. L. M'Sabah, M. Boucharef, J. Warnan, Y. Pellegrin, E. Blart, B. Lucas, F. Odobel and J. Bouclé, *Phys. Chem. Chem. Phys.*, 2015, **17**, 9910–9918.
26 G. Kodis, Y. Terazono, P. A. Liddell, J. Andréasson, V. Garg, M. Hambourger, T. A. Moore, A. L. Moore and D. Gust, *J. Am. Chem. Soc.*, 2006, **128**, 1818–1827.
27 F. Matino, V. Arima, M. Piacenza, F. Della Sala, G. Maruccio, R. J. Phaneuf, R. Del Sole, G. Mele, G. Vasapollo, G. Gigli, R. Cingolani and R. Rinaldi, *Chemphyschem*, 2009, **10**, 2633–2641.

28 K. J. Elliott, A. Harriman, L. L. Pleux, Y. Pellegrin, E. Blart, C. R. Mayer and F. Odobel, *Phys. Chem. Chem. Phys.*, 2009, **11**, 8767–8773.

29 G. Bottari, O. Trukhina, M. Ince and T. Torres, *Coord. Chem. Rev.*, 2012, **256**, 2453–2477.

30 G. N. Lim, E. Maligaspe, M. E. Zandler and F. D'Souza, *Chemistry*, 2014, **20**, 17089–17099.

31 S. Fukuzumi, K. Ohkubo and T. Suenobu, *Acc. Chem. Res.*, 2014, **47**, 1455–1464.

32 E. J. Ngen, L. Xiao, P. Rajaputra, X. Yan and Y. You, *Photochem. Photobiol.*, 2013, **89**, 841–848.

33 J.-Z. Lu, X.-C. Tan, J.-W. Huang, C.-H. Dong, B. Fu, H.-C. Yu and L.-N. Ji, *Transit. Met. Chem.*, 2005, **30**, 643–649.

34 X. Sun, D. Li, G. Chen and J. Zhang, *Dyes Pigments*, 2006, **71**, 118–122.

35 P. G. Seybold and M. Gouterman, *J. Mol. Spectrosc.*, 1969, **31**, 1–13.

36 R. G. Little, J. A. Anton, P. A. Loach and J. A. Ibers, *J. Heterocycl. Chem.*, 1975, **12**, 343–349.

37 D. Monti, M. Venanzi, G. Mancini, F. Marotti, L. La Monica and T. Boschi, *Eur. J. Org. Chem.*, 1999, **1999**, 1901–1906.

38 M. Taniguchi, H. Du and J. S. Lindsey, *J. Chem. Inf. Model.*, 2011, **51**, 2233–2247.

39 B. Boëns, P.-A. Faugeras, J. Vergnaud, R. Lucas, K. Teste and R. Zerrouki, *Tetrahedron*, 2010, **66**, 1994–1996.

40 A. Nowak-Król, R. Plamont, G. Canard, J. A. Edzang, D. T. Gryko and T. S. Balaban, *Chem. - Eur. J.*, 2015, **21**, 1488–1498.

41 F. Himo, T. Lovell, R. Hilgraf, V. V. Rostovtsev, L. Noodleman, K. B. Sharpless and V. V. Fokin, *J. Am. Chem. Soc.*, 2005, **127**, 210–216.

42 T. L. C. Figueiredo, R. A. W. Johnstone, A. M. P. S. Sørensen, D. Burget and P. Jacques, *Photochem. Photobiol.*, 1999, **69**, 517–528.

43 S. A. P. Guarìn, D. Tsang and W. G. Skene, *New J. Chem.*, 2007, **31**, 210–217.

44 I. Singh, C. Freeman and F. Heaney, *Eur. J. Org. Chem.*, 2011, **2011**, 6739–6746.

45 R. Huisgen, *Angew. Chem. Int. Ed. Engl.*, 1963, **2**, 565–598.

46 R. Huisgen, *Angew. Chem.*, 1963, **75**, 604–637.

47 C. W. Tornøe, C. Christensen and M. Meldal, *J. Org. Chem.*, 2002, **67**, 3057–3064.

48 M. Gouterman, *J. Mol. Spectrosc.*, 1961, **6**, 138–163.

49 R. Bonnett, D. J. McGarvey, A. Harriman, E. J. Land, T. G. Truscott and U.-J. Winfield, *Photochem. Photobiol.*, 1988, **48**, 271–276.

50 M. O. Senge, *Chem. Commun.*, 2006, 243–256.

51 G. C. Tron, T. Pirali, R. A. Billington, P. L. Canonico, G. Sorba and A. A. Genazzani, *Med. Res. Rev.*, 2008, **28**, 278–308.

52 J.-D. Chai and M. Head-Gordon, *Phys. Chem. Chem. Phys.*, 2008, **10**, 6615–6620.

53 J.-D. Chai and M. Head-Gordon, *J. Chem. Phys.*, 2008, **128**, 084106.

54 Y. Kodama, K. Nishihata, M. Nishio and N. Nakagawa, *Tetrahedron Letters*, 1977, **18**, 2105–2108.

55 K. Shibasaki, A. Fujii, N. Mikami and S. Tsuzuki, *J. Phys. Chem. A*, 2006, **110**, 4397–4404.

56 M. Albertí, A. Aguilar, F. Huarte-Larrañaga, J. M. Lucas and F. Pirani, *J. Phys. Chem. A*, 2014, **118**, 1651–1662.

57 M. Gouterman, G. H. Wagnière and L. C. Snyder, *J. Mol. Spectrosc.*, 1963, **11**, 108–127.

58 D. Marsh and L. Mink, *J. Chem. Educ.*, 1996, **73**, 1188.

59 W. M. F. Fabian, S. Schuppler and O. S. Wolfbeis, *J. Chem. Soc. Perkin Trans. 2*, 1996, 853–856.

60 K. A. Nguyen, P. N. Day and R. Pachter, *J. Phys. Chem. A*, 1999, **103**, 9378–9382.

61 M. Dulski, M. Kempa, P. Kozub, J. Wójcik, M. Rojkiewicz, P. Kuś, A. Szurko, A. Ratuszna and R. Wrzalik, *Spectrochim. Acta. A.,* 2013, **104**, 315–327.

62 M.-J. Zhang, Y.-R. Guo, G.-Z. Fang and Q.-J. Pan, *Comput. Theor. Chem.*, 2013, **1019**, 94–100.

63 T. Yanai, D. P. Tew and N. C. Handy, *Chem. Phys. Lett.*, 2004, **393**, 51–57.

64 L. Poulsen, M. Jazdzyk, J.-E. Communal, J. C. Sancho-García, A. Mura, G. Bongiovanni, D. Beljonne, J. Cornil, M. Hanack, H.-J. Egelhaaf and J. Gierschner, *J. Am. Chem. Soc.*, 2007, **129**, 8585–8593.

65 R. E. Di Paolo, J. Seixas de Melo, J. Pina, H. D. Burrows, J. Morgado and A. L. Maçanita, *ChemPhysChem*, 2007, **8**, 2657–2664.

66 A. B. Ormond and H. S. Freeman, *Dyes Pigments*, 2013, **96**, 440–448.

67 G. Weber and F. W. J. Teale, *Trans. Faraday Soc.*, 1958, **54**, 640–648.

68 R. Sjöback, J. Nygren and M. Kubista, *Spectrochim. Acta. A. Mol. Biomol. Spectrosc.*, 1995, **51**, L7–L21.

69 Y. Yang, M. N. Weaver and K. M. Merz, *J. Phys. Chem. A*, 2009, **113**, 9843–9851.

70 M. J. Frisch, G. W. Trucks, H. B. Schlegel, G. E. Scuseria, M. A. Robb, J. R. Cheeseman, G. Scalmani, V. Barone, B. Mennucci, G. A. Petersson, H. Nakatsuji, M. Caricato, X. Li, H. P. Hratchian, A. F. Izmaylov, J. Bloino, G. Zheng, J. L. Sonnenberg, M. Hada, M. Ehara, K. Toyota, R. Fukuda, J. Hasegawa, M. Ishida, T. Nakajima, Y. Honda, O. Kitao, H. Nakai, T. Vreven, J. A. Montgomery, Jr., J. E. Peralta, F. Ogliaro, M. Bearpark, J. J. Heyd, E. Brothers, K. N. Kudin, V. N. Staroverov, R. Kobayashi, J. Normand, K. Raghavachari, A. Rendell, J. C. Burant, S. S. Iyengar, J. Tomasi, M. Cossi, N. Rega, N. J. Millam, M. Klene, J. E. Knox, J. B. Cross, V. Bakken, C. Adamo, J. Jaramillo, R. Gomperts, R. E. Stratmann, O. Yazyev, A. J. Austin, R. Cammi, C. Pomelli, J. W. Ochterski, R. L. Martin, K. Morokuma, V. G. Zakrzewski, G. A. Voth, P. Salvador, J. J. Dannenberg, S. Dapprich, A. D. Daniels, O. Farkas, J. B. Foresman, J. V. Ortiz, J. Cioslowski and D. J. Fox, *Gaussian 09, Revision A.1*, Gaussian, Inc., Wallingford, CT, 2009.

View Article Online
DOI: 10.1039/C5NJ02901E

Modulations of optical properties of a new porphyrin-fluorescein dyad were elucidated by experimental and theoretical techniques, conformational rearrangements being studied.